Hepatic Progenitor Cells Promote the Repair of Schistosomiasis Liver Injury Through Inhibiting IL-33 Secretion

Beibei Zhang
Xuzhou Medical University
Xiaoying Wu
Third Affiliated Hospital of Sun Yat-Sen University
Jing Li
Xuzhou Medical University
An Ning
Jiangxi provincial Institute of Parasitic Diseases
Bo Zhang
Xuzhou Medical University
Jiahua Liu
Sun Yat-sen University Zhongshan School of Medicine
Langui Song
The Eighth Affiliated Hospital of Sun Yat-Sen University
Chao Yan
Xuzhou Medical University
Xi Sun
Sun Yat-sen University Zhongshan School of Medicine
Kuiyang Zheng (zky@xzhmu.edu.cn)
Jiangsu Key Laboratory of Immunity and Metabolism, Department of Pathogenic Biology and Immunology, Xuzhou, Jiangsu, China
Zhongdao Wu
Sun Yat-sen University Zhongshan School of Medicine

Research

Keywords: hepatic schistosomiasis, hepatic progenitor cells, IL-33

DOI: https://doi.org/10.21203/rs.3.rs-137173/v1

Abstract

Background: Hepatic schistosomiasis, a chronic liver injury induced by long-term *Schistosoma japonicum* (*S. japonicum*) infection, is characterized by egg granulomas and fibrotic pathology. Hepatic progenitor cells (HPCs), which are nearly absent and quiescent in normal liver, play vital roles in chronic and severe liver injury. But their role in the progression of liver injury during infection remained unknown.

Methods: In this study, the hepatic egg granulomas, fibrosis and proliferation of HPCs were analyzed in *S. japonicum* infection mice model at different infection stages. For validating the role of HPCs in hepatic injury, TNFrelated weak inducer of apoptosis (TWEAK) and TWEAK blocking antibody were used to manipulate the proliferation of HPCs. Histologic pathology and the expression of IL-33 were examined.

Results: We found that the proliferation of HPCs paralleled with inflammatory granulomas and fibrosis formation. Promoting HPCs expansion promote the liver regeneration and inhibit the hepatocytes injury, the inflammatory eggs granulomas and the deposition of fibrotic collagen. Interestingly, the expression of IL-33 decreased when HPCs were manipulated to proliferate. Thus, IL-33 might be involved in the liver repair dominated by HPCs.

Conclusions: Collectively, our data uncovered a protective role of HPCs in hepatic schistosomiasis in an IL-33 related manner, which might provide a promising progenitor cell therapy for hepatic schistosomiasis.

Introduction

Schistosomiasis is one of the main human helminth infection that is responsible for liver injury. China is the main epidemic area of schistosomiasis japonica[1]. By 2018, there are still 29,214 patients with advanced schistosomiasis in China[2]. The most common pathological consequences in schistosomiasis are associated with chronic disease and are dominated by a Th2 immune response to the continuous stimulation of soluble egg antigen[3]. A granulomatous response was initiated by inflammatory cells infiltration around trapped eggs. And secondary fibrosis is arisen by fibroblasts activation and collagen fibers deposition with the granuloma maturing. Meanwhile, hepatocyte apoptosis and necrosis inevitably occurred at the same time. Without efficient treatment, hepatic schistosomiasis can result in morbidity and even mortality[1]. Lots of researches have been conducted for elaborating the mechanism and repair of liver injury in schistosomiasis japonica, but still remains largely unknown.

Adult stem/progenitor cells are vital for maintaining organ homeostasis under chronic pathological conditions. The stem/progenitor cells therapy has been largely studied and is likely to be a promising treatment for multiple organ injury[4]. Many studies reported that the evolution of HPCs not only contribute to the regenerative and reparative response, but also inevitably correlates with the fibrotic process. The functions of HPCs in many human hepatic diseases or mouse models have been

investigated[5]. However, to date, it is unclear whether HPCs modulate the liver injuries induced by *S. japonicum* infection.

The activation of HPCs is associated with the degree of inflammation and fibrosis. It is well known that the expansion and differentiation of HPCs are dependent on interaction with hepatic stellate cells (HSCs), macrophages and extracellular matrix (ECM)[6]. Notably, macrophages and HSCs have been reported to be two key cellular components that contribute to the inflammatory granulomas, collagen fibers deposition and the formation of fibrosis in schistosomiasis japonica[7, 8] All these indicate that HPCs can probably be activated in the process of this infectious disease. This study aimed to clarify the role and mechanism of HPCs in liver pathological regulation and repair. We found that the expansion of HPCs suppressed the development of the hepatic granulomas and fibrosis in infected mice. Moreover, IL-33 was involved in HPCs-mediated liver injury repair.

Materials And Methods

Mice model

Six to eight weeks old male BALB/c mice were purchased from the Experimental Animal Center of Guangdong Province. They were supplied with sterile food and water ad libitum and housed in the Biosafety Level-2 (BSL-2) laboratory of Sun Yat-sen University with 21–26℃ room temperature, 40–70% humidity and 12 hours light/ dark cycle. All the procedures of animal experiments and reporting follow to the ARRIVE guidelines. Mice were infected with *S. japonicum* after at least one-week acclimatization.

We purchased the *Oncomelania hupehensis* (*O.hupehensis*) snails infected with cercariae from the National Institute of Parasitic Diseases, Chinese Center for Disease Control and Prevention in Shanghai. *O. hupehensis* snails were put into water without chlorine under light to release cercariae. To infect mice with cercariae, 15 ± 2 cercariae were picked onto a glass slide under the anatomical microscope and the glass was placed on the abdomen of a mouse for 15 minutes. After 4, 6, 10 and 14 weeks, control mice without infection and infected mice were sacrificed under deep anesthesia with 2% pentobarbital at a dose of 45 mg/kg.

After 4 weeks of infection, for activating HPCs *in vivo*, mice were subjected with 20 μg/kg of the recombinant TNFrelated weak inducer of apoptosis (TWEAK) (R&D,1237-TW/CF, Minneapolis, Minnesota, USA) or phosphate-buffered saline (PBS) as control via tail intravenous injection. For inhibition the activation of HPCs using 2 mg/kg TWEAK blocking antibody (Biolegend, 120008, San Diego, CA, USD) or 2 mg/kg isotype control antibody (Biolegend, 400427, San Diego, CA, USD) via tail intravenous injection. All doses used were followed the manufactures instructions and all injections were conducted twice a week for two weeks or five weeks.

Serum Albumin and IL-33 assay

Blood was collected and rest at room temperature for 2 hours. After centrifuging at 4000 g for 10 minutes, the serum was separated and transferred to other tubes. One part with 200 μl was sent to KingMed Diagnostics Co., Ltd. (Guangzhou, China) for measuring the concentration of albumin. For detecting IL-33 in serum, an enzyme-linked immunosorbent assay (ELISA) kit was obtained (Invitrogen, 88-7333-22, Massachusetts, United States) and the assay was performed according to the manufacture's instructions.

Liver pathology measurement and immunohistochemistry analysis

The liver tissues were cut into 2 × 2 × 0.3 cm^3 and fixed in 4% paraformaldehyde according to standard protocols. Then, samples were cut into 4-μm-thick continuous sections. Hematoxylin and eosin (H&E) staining and Masson trichrome staining were used for evaluating the percents of granulomas and fibrosis area, respectively. All these sections were scanned by a Zeiss Axio Scan.Z1 microscope (Carl Zeiss AG, Oberkochen, Germany) and the whole image of each section obtained was analyzed by Image Pro Plus 6.0 software.

HPCs proliferation was assessed by immunohistochemistry (IHC). In detail, all de-waxed sections were kept in boiling citrate solution for half an hour. After blocking the endogenous peroxidase activity with methanolic hydrogen peroxide (3%) for 10 minutes at room temperature, sections were incubated with 1% BSA for 30 minutes for blocking nonspecific antigen epitopes and incubated with primary A6 antibody (obtained from Developmental Studies Hybridoma Bank), CK19 antibody (Abcam, ab194399,Cambridge, UK), Epcam antibody (Abcam, ab213500, Cambridge, UK), F4/80 (CST, #30325, Darmstadt, Germany) antibody and CD45 (Proteintech, 60287-1-Ig, Wuhan, China) antibody at 4 ℃ overnight. After washing three times with PBS, 50 μl of ready-to-use HRP labelled anti-mouse/rabbit general secondary antibodies (Dako, Copenhagen, Denmark) was added to each section and incubated for half an hour at room temperature. Finally, each section was observed under a light microscope when 3,3'-diaminobenzidine (DAB) substrate was added and the reaction was stopped by putting the section into distilled water for 6 minutes. After sections were counterstained with hematoxylin and dehydrated, sections were mounted with neutral gum. For assessing the HPCs compartment, all sections were scanned by a Zeiss Axio Scan.Z1 microscope (Carl Zeiss AG, Oberkochen, Germany) and we can get the image of the whole tissue (original magnification, × 100). The positive HPCs within the bile/reactive ductules and the solitary or clumped A6- or CK19- or Epcam-positive HPCs that were present at the portal interface or in the parenchyma were counted. But cholangiocytes locating on the side of the lumen of the interlobular bile ducts were excluded from the counts. The number of HPCs was shown as the number of CK19- or Epcam-positive cells per field. For each group, at least four samples were analyzed[9, 10].

TUNEL assay

The apoptosis of hepatocytes were detected by TUNEL staining with an In Situ Cell Death Detection Kit (Roche, Switzerland). All the procedures were strictly according to the manufacture's instructions. Briefly, paraformaldehyde-fixed tissue sections were dewaxed and subsequently incubated with proteinase K at

27 ℃ for 25 min. After washing 3 times, permeabilization solution containing 0.1% Triton X–100 and 0.1% sodium citrate were added and kept for 8 min. Then, a 50 μl TUNEL reaction mixture was added. 50 μl label solution and DNase I recombinant were added in the negative control and positive control, respectively. All samples were incubated for 60 min at 37 ℃ in a humidified incubator in the dark. Lastly, one drop of DAPI was added and kept for 5 min. After washing 3 times with PBS, all slides were covered with an anti-fluorescence quenching agent and captured under an Olympus BX-63 microscopy (Olympus, Tokyo, Japan). For each group, at least four samples were analyzed.

Hydroxyproline

Liver tissues (40–50 mg) were weighed precisely for measuring the content of hydroxyproline. All the procedures have followed the instructions of a commercially hydroxyproline assay kit (Jiancheng Institute of Biotechnology, A030-2, Nanjing, China). The OD value of each sample was read by a Tecan Sunrise system (Sunrise, TECAN, Männedorf, Austria) and the content of hydroxyproline was calculated according to the formula listed in the instructions.

RNA extraction, cDNA Synthesis and Real-time PCR

Total RNA was isolated from the liver tissue using Trizol reagent (Invitrogen, New York, United States) following the manufacture's protocols. The quantity and quality of the RNA were estimated by a NanoDrop 2000 spectrophotometer (Thermo Fisher Scientific, 78441, Massachusetts, United States). Then, 3 μg RNA was reversed transcribed using a cDNA Synthesis Kit (Thermo Fisher Scientific, 78441, Massachusetts, United States). The expression levels of *HGF* mRNA, *IL-6* mRNA, *α-SMA* mRNA, *Collagen-I* mRNA, *IL-33* mRNA and *GAPDH* mRNA were detected using SYBR Premix Ex TaqTM (TaKaRa, Osaka, Japan) and the specific primers pairs were listed in Table 1. The reaction procedure was followed as described previously[11] and performed with a CFX 96 touch instrument (Bio-Rad, CA, United States). The *GAPDH* mRNA level was used for normalization. All the relative mRNA levels were calculated using the $2^{-\Delta\Delta CT}$ method and normalized to the control group.

Table 1
Primers used for Real-time PCR

Genes	Primer	Sequence(5'-3')
GAPDH	Forward primer	ACTCCACTCACGGCAAATTC
	Reverse primer	TCTCCATGGTGGTGAAGACA
HGF	Forward primer	CCAGAGGTACGCTACGAAGT
	Reverse primer	CTGTGTGATCCATGGGACCT
IL-6	Forward primer	GACTGATGCTGGTGACAACC
	Reverse primer	AGACAGGTCTGTTGGGAGTG
α-SMA	Forward primer	CACAGCCCTGGTGTGCGACAAT
	Reverse primer	TTGCTCTGGGCTTCATCCCCCA
Collagen-I	Forward primer	TCCTGCGCCTAATGTCCACCGA
	Reverse primer	AAGCGACTGTTGCCTTCGCCTC
IL-33	Forward primer	ACACAGTCTCCTGCCTCCCT
	Reverse primer	CCACACCGTCGCCTGATTGA

Western blotting

Total protein was extracted from 30–50 mg liver tissue using an extraction buffer containing RIPA lysis buffer (Thermo Fisher Scientific, 89901, Massachusetts, United States) and protease and phosphatase inhibitors cocktails (Thermo Fisher Scientific, 78441, Massachusetts, United States). A total of 50 μg protein was separated on an SDS-polyacrylamide gel with 120 V for 2 hours and transferred to a PVDF membrane with 100 mA for 3 hours on ice. Then, the PVDF membrane was blocked in 5% nonfat milk in TBST for 2 hours at room temperature and incubated with mouse anti-IL-33 antibody using at 1:1000 dilution (Abcam, ab54385, Cambridge, England) and mouse anti-GAPDH antibody using at 1:2000 dilution (Sigma-Aldrich, G8795, St. Louis, MO, United States,) overnight at 4 ℃. Anti-mouse IgG (Santa Cruz, 7076S, CA, United States) was diluted at 1:5000 ratio and used as a secondary antibody. After washing 3 times with TBST, membrane was incubated with a secondary antibody for 1 hour at room temperature. After adding ECL substrate (Millipore, MA, United States), the protein band was visualized and captured with an Amersham Imager 600 system (GE, CT, United States). The density of the band was quantified by an Image J2x software and normalized to GAPDH.

Isolation of hepatocytes, HSCs and macrophages

Livers were perfused with 37℃ PBS at a rate of 2 ml/min for 5 min to flush the blood out of the livers and digested in situ subsequently with 37 ℃ 0.04% collagenase type IV (gibco,Massachusetts, United States) at a rate of 2 ml/min for 8 min. Then, livers were removed and tore into pieces. After keeping

digesting for 6 min in 37℃, the digestion was added cold DMEM containing 20% FBS to stop digesting and filtered through a 70 μm membrane into a 50 ml tube. The supernatant was centrifuged at 500 g for 5 min at 4 ℃. The cell pellet was resuspended and centrifuged at 50 g for 4 min. The hepatocytes sunk to the bottom of the tube, and nonparenchymal cells remained in the supernatant. The supernatant was recentrifuged at 500 g for 7 min, and the supernatant was removed carefully. The cell pellet was added 12% and 18% iodixanol gradient (OptiPrep; Axis-Shield PoC AS, Oslo, Norway) and centrifuged at 1400 g without brakes for 20 min. So, we can get the HSCs and macrophages. To get high purified cells, fluorescence-activated cell sorting was used. The CD 11b positive cells were referred as macrophages and negatives cells as HSCs. FACS-Calibur analysis demonstrated that the purities of HSCs and macrophages were > 90% purity.

Statistical Analysis

Quantitative data were shown as Mean ± SEM. Statistical significance was analyzed with SPSS 19.0 software. Comparisons between two groups were determined with independent-sample *t*-test, and significances between multiple groups were determined by one-way ANOVA followed by LSD or non-parametric test followed by Kruskal-Wallis H test. $P < 0.05$ were considered as statistically significant.

Results

Liver regeneration got involved in the alleviation of liver injury induced by infection

The liver has a remarkable regeneration capacity after injury. To investigate whether liver regeneration occurred in mice following infection, liver samples were collected at different infection stages. By HE and Masson staining, we noted that the liver showed slightly inflammatory cells infiltration and fibrotic formation at 4 weeks post-infection (wpi), but, inflammatory granulomas and fibrosis area increased sharply at 6 wpi ($P < 0.001$). Interestingly, those started to decrease from 10 wpi to 14 wpi (Fig. 1A-D). Meanwhile, there were no necrosis and apoptotic hepatocytes at 4 wpi. Large numbers of necrotic cells and apoptotic hepatocytes appeared around the granulomas at 6 wpi, but reduced significantly after 10 wpi (Fig. 1E). This pattern was similar to inflammatory and fibrotic status. The CD45 positive inflammatory cells (Fig. 1F) and F4/80 (Fig. 1G) positive cells also increased significantly at 6 wpi and decreased after 10 weeks of infection. All these implied that in a single infection mouse model, the liver histopathology, including inflammatory granulomas and fibrosis, could be self-recovery. Notably, compared with the uninfected and 4 wpi groups, the level of hepatocytes marker albumin in blood decreased significantly at 6 wpi. But, with the liver pathology relieving after 10 wpi, the albumin increased gradually (Fig. 1H). Thus, we suspected that liver regeneration might get involved in this process.

The expansion of HPCs was induced in mice with infection

Following liver injury, HPCs have been reported to play potential roles in liver repopulation and regeneration[12]. We wondered whether HPCs contributed to self-recovery via promoting liver regeneration in hepatic schistosomiasis. HPCs marker A6, CK19, and Epcam were detected by IHC. As results showed in Fig. 2A and Fig. 2D, the level of A6 was higher than the uninfected group, and it remained high level until 14 wpi ($P < 0.001$). In addition, CK19 and Epcam also increased at 6 wpi ($P < 0.001$) and kept increasing after 10 wpi (Fig. 2B, 2C, 2E and 2F). We also tested the HPCs related cytokines *HGF* mRNA (Fig. 2G) and *IL-6* mRNA (Fig. 2H) expression profiles. The mRNA of *HGF* upregulated sharply at 10 wpi and kept at a high level at 14 wpi. For *IL-6* mRNA, it was higher upon 6 wpi than the uninfected group and lasted for 14 weeks. This data indicated that the activation and proliferation of HPCs occurred when the inflammatory granulomas and fibrosis outbroke.

HPCs promoted the repair of liver injury induced by S. japonicum **infection**

To clarify whether HPCs mediate liver regeneration and thus modulate the repair of liver injury in *S. japonicum* infected mice, TWEAK, a specific mitogen for the proliferation of HPCs, was used to experimentally manipulate the proliferation of HPCs. TWEAK-neutralizing antibody was used to inhibit the proliferation of HPCs. PBS and isotype antibody were used as control. At 6 wpi, there were no apparent differences in the expression of A6, CK19 and Epcam between the isotype and anti-TWEAK treatment mice with infection (Fig. 3A-3F). All these markers were higher in the rh-TWEAK treated group than the PBS and rh-TWEAK treated groups. At 9 wpi, compared with the infected group with PBS treatment, A6($P < 0.01$), CK19 ($P < 0.05$) and Epcam ($P < 0.05$) were higher in rh-TWEAK treated group. Conversely, A6 ($P < 0.001$), CK19 ($P < 0.01$) and Epcam ($P < 0.001$) decreased significantly in anti-TWEAK group. These data approved that rh-TWEAK induced the activation and proliferation of HPCs, while blocking antibody inhibited HPCs response successfully. Furthermore, At 9 wpi, the serum albumin improved significantly with rh-TWEAK treatment (Fig. 3G). But it remained unchanged when infected mice were treated with anti-TWEAK. Thus, proliferated HPCs might contribute to liver regeneration via differentiating into hepatocytes.

To address whether the proliferation of HPCs modulated the liver injury, HE and Masson staining were conducted to determine the inflammatory granulomas and fibrosis (Fig. 4A-4D). At 6 wpi, these showed no apparent differences among the four infected groups. But at 9 wpi, in contrast to Sj-PBS and Sj-Iso groups, the percent of granulomas area and fibrosis area decreased obviously in infected livers with HPCs expansion. Conversely, it increased obviously in infected livers with a reduced expansion of HPCs. We also detected the content of hydroxyproline (Fig. 4E) and pro-fibrotic genes α-SMA (Fig. 4F) and Collagen-I (Fig. 4G), and they showed similar trends with HE and Masson staining. Additionally, we found that the necrosis of hepatocytes was serious in these four infected groups at 6 wpi and alleviated at 9 wpi. It was relatively milder in Sj-rh-TWEAK group and more severe in Sj-anti-TWEAK group (Fig. 4A and 4H). Thus, HPCs expansion can inhibit hepatocytes injury by differentiating into new hepatocytes, and then replenishing the necrosis of hepatocytes. To conclude, the proliferation of HPCs can inhibit the formation of granulomas, fibrosis and promote hepatocytes regeneration in *S. japonicum* infected mice.

HPCs inhibited IL-33 secretion in S. japonicum infection mice

IL-33 is an important inflammatory cytokine, which can promote the hepatic fibrosis through mediating shrift to Th2 paradigm[13]. In this single infection mouse model with, it was found that the protein and mRNA levels of IL-33 elevated sharply at 6 wpi (Fig. 5). This high expression remained until 14 wpi. Then we sought to clarify whether HPCs can modulate the section of IL-33. Interestingly, promoting HPCs proliferation resulted in decreased expression of IL-33. On the contrary, it was higher when the proliferation was inhibited (Fig. 6A-6C). Besides, we detected the concentration of IL-33 in serum, which slightly increased in HPCs proliferated group, but strikingly augmented when HPCs proliferation was inhibited ($P < 0.01$). This finding suggested the HPCs' role in promoting the repair of hepatic schistosomiasis might be through inhibiting IL-33 secrection.

IL-33 was identified to be produced by some endothelial, epithelial cells and some hematopoietic cells including macrophage[14]. HSCs and macrophages are two major cellular components contributing to the liver injury in schistosomiasis japonica[3]. In this study, HSC and macrophage were isolated from normal and infected livers. The mRNA level of IL-33 was determined. As the result shown in Fig. 6E, IL-33 could be detected in HSC isolated from infected liver. But it decreased when HPCs were manipulated to proliferate ($P < 0.05$). In contrast, inhibiting the proliferation of HPCs upregulated the mRNA level of IL-33 in HSCs. However, the expression of IL-33 in macrophages kept at a base level and showed no changes regardless of the population of HPCs. All these data indicated that HPCs might alleviate the liver injury via inhibiting the expression of IL-33, which especially in HSCs.

Discussion

The liver is special for its remarkable regenerative ability after tissue loss[15]. In a single infection mouse model with *S. japonicum*, the expansion of HPCs contributed to the hepatocytes regeneration. It inhibited the formation of inflammatory egg granulomas and secondary fibrosis. Moreover, we identified that the regulatory function of HPCs was partly through inhibiting the secretion of IL-33 from HSCs. Thereby, we firstly revealed the role and mechanism of HPCs playing in hepatic schistosomiasis japonica, which was important for understanding the pathogenic mechanism and developing a new strategy for this liver disease.

Chronic hepatic schistosomiasis results from long-standing infections with massive collagen deposition in the periportal space and tremendous inflammatory cell infiltration[1]. Though it can lead to unreversible fibrosis and even cirrhosis, the hepatocellular function remains nearly at a normal level[16]. In this study, we found that inflammatory granulomas, fibrosis, and hepatocytes injury can not be observed before 4 wpi. But all these pathological changes outbroke at 6 wpi and ameliorated significantly with the lastingness of infection. It implied that liver injury induced by *S. japonicum* infection could repair itself. Moreover, the necrosis and apoptosis of hepatocytes were found to be serious at 6 wpi, which obviously impoved at 10 wpi. Intriguingly, we found that hepatocytes regeneration occurred after 10 wpi through monitoring the level of albumin, a marker of hepatocytes, so the damaged hepatocytes driven by *S.*

japonicum infection can be replenished by these newborn cells. Therefore, our data revealed that the liver function remained largely unaffected due to efficient cell regeneration.

Liver regeneration after tissue injury involves the supplement from several cell types[17]. With the developing of regenerative medicine, a population of cells residing within the distal part of the bile duct (also called the canals of Hering) was identified as endogenous stem cells in the liver[18]. It posses bipotential differentiation capacity, which can replace hepatocytes or cholangiocytes during regeneration. Notably, the mechanism of regeneration varies in different liver diseases and disease at different stages [19, 20]. In conditions with steady status, the homeostasis is maintained by mature hepatocytes. But the regeneration was dominated by activated HPCs in the liver with prolonged injury or massive hepatocytes and cholangiocytes loss[21]. In *S. japonicum* infection mice model, we found that the proliferation of HPCs upregulated after 6 wpi. It was no accident that the collagen deposition, CD45, and F4/80 all increased concurrently. These represented the activation of the HSCs, accumulation of macrophages and liver inflammatory response. It was well studied that HSCs and invading macrophages were important determinants of HPCs expansion[22, 23]. They can provide pro-mitogenic factors such as HGF, TGF-β, TNF-α, and IL-6[21]. More importantly, activation of the Notch signalling pathway by HSC and Wnt/β-catenin signalling pathway was vital for the differentiation of HPCs[24, 25].In contrast to 10 wpi, HPCs increased slightly at 6 wpi, which was an acute stage for infection in mice. Therefore, HPCs might take part in the repair of hepatic injury at the chronic stage.

To confirm the function of HPCs playing in hepatic schistosomiasis, TWEAK, a specific mitogen for HPCs was used to manipulate the proliferation of HPCs. We found that the expansion of HPCs alleviated the inflammatory granuloma and fibrosis efficiently. Additionally, it facilitated the hepatocytes regeneration, which can be implied by the downregulated necrosis and apoptosis of hepatocytes and increased expression of hepatocytes marker albumin at the later infection stage. Even though rh-TWEAK was injected at 4 wpi, the expansion of HPCs could not inhibit the progress of liver injury at 6 wpi. We deemed that HPCs could not define against the drastic pathogenicity of eggs at the acute stage. But with the continuous expansion of HPCs induced by rh-TWEAK, they can effectively prevent liver injury at 9 wpi. Professor Xu and his colleagues reported that Mesenchymal stem cells could ameliorate fibrosis in infected mouse[26]. Although MSCs have been reported to be used in the clinic for several cases, samples size of MSCs on liver transplantation for clinical trials is insufficient. To date, there are several main obstacles for MSCs application in liver transplantation: ethical doubt, safety concerns, systemic immunosuppression, sources of MSCs, time delays and high costs for the generation and handling of MSCs[27, 28]. Besides, the truth is that most of the patient with schistosomiasis live in remote and economically backward regions[16]. It is too expensive for them to receive liver transplantation with stem cells. Our data suggested that specific mitogen TWEAK could facilitate the proliferation of liver endogenous stem/progenitor cells HPCs. Then, proliferated HPCs promote the repair of the liver injury sufficiently. Therefore, our work might supply a potential effective and economical therapy for schistosomiasis, but further researches are needed.

IL-33, a member of the IL-1 family, plays an important role in both innate immune and adaptive immune. It was a key mediator in Th2 associated inflammatory disorders[29]. IL-33/ST2 axis gets involved in the pathogenesis of liver injuries, such as viral hepatitis, acute hepatitis, and fatty liver disease[30]. Our data show that IL-33 significantly increased in infected mice. Moreover, our team has previously clarified that IL-33 contributed to schistosomiasis japonica via inducing M2 macrophages polarization[31]. Pan and his colleagues reported that miR-203-3P from the liver promoted the *S. japonicum*-induced hepatic pathology by targetting IL-33 in HSCs[32]. In our study, we found that HPCs proliferation led to a decrease in IL-33 level. In contrast, IL-33 increased markedly when the proliferation of HPCs was inhibited. Considering that HSCs and macrophages are two main cell components contributing to hepatic schistosomaisis[3], we analyzed the IL-33 in both of these two cell types. Interestingly, it displayed that the proliferation of HPCs negatively affected the expression of IL-33 in HSCs but not in macrophages. This reconfirmed that there is an interaction between HPCs and HSCs[33]. Our future study will focus on exploring how HPCs regulate the expression of IL-33 in HSCs. All these results suggested that HPCs modulated the liver histopathology in an IL-33 dependent manner.

Conclusions

Taken together, we verified a protective role of IL-33-dependent HPCs response in liver injury induced by *S. japonicum* infection. Our work supply a basic framework for further study of the therapeutic benefits of HPCs in the treatment of hepatic schistosomiasis japonica.

Abbreviations

S. japonicum
Schistosoma japonicum; HPCs:hepatic progenitor cells; TWEAK:TNFrelated weak inducer of apoptosis; HSCs:hepatic stellate cells; ECM:extracellular matrix; BSL-2:Biosafety Level-2; *O. hupehensis*:*Oncomelania hupehensi* ; ELISA:Enzyme-linked immunosorbent assay; H&E:Hematoxylin and eosin; IHC:immunohistochemistry; CK19:cytokeratin 19; Epcam:Epidermal cell adhesion molecule; HGF:hepatocyte growth factor; TNF:tumor necrosis factor; TGF:transforming growth factor.

Declarations

Acknowledgements

The authors thank the Chinese Center for Disease Control and Prevention for supplied us with cercariae positive *Oncomelania hupehensis* (*O. hupehensis*) and Koda Stephane for editing our manuscript.

Authors' contributions

BBZ, ZDW and KYZ conceived the study and participated in the study design. ZBB, XYW, JL, AN, BZ and JHL performed the research performance. ZBB wrote this manuscript. LGS, XS and CY revised the

manuscript. ZDWand KYZ reviewed the final version of the manuscript and supervised the project. All authors read and approved the final version of the manuscript.

Funding

Funding

This work was supported by the National Natural Science Foundation of China (Grant Numbers: 81871682, 81601781), Natural Science Foundation of Jiangsu Province of China (Grant No. BK20201011), Natural Science Research of Jiangsu Higher Education Institutions of China (Grant No. 20KJB310011), Jiangsu Postdoctoral Science Foundation (Grant No. RC7062005), Xuzhou Medical University Scientific Research Foundation for Outstanding Talents (D2019040) and Postgraduate Innovation Program of Xuzhou Medical University (KYCX20-2468). The funders had no role in study design, data collection, analysis, decision to publish and preparation of the manuscript.

Availability of data and materials

All the data used to support the findings of this study are included in this manuscript, and the original files can be available from the corresponding author upon reasonable request.

Ethics approval and consent to participate

All animal experiments were strictly carried out under the National Guidelines for Experimental Animal Welfare (MOST, China, 2006) and with ethical permission from the Institutional Animal Care and Use Committee of Sun Yat-sen University (Permit No: 2016-104).

Consent for publication

All the authors are consented to publish.

Competing interests

The authors declare that they have no competing interests.

References

[1] McManus DP, Dunne DW, Sacko M, Utzinger J, Vennervald BJ, Zhou XN. Schistosomiasis. Nat Rev Dis Primers. 2018;4(1):13.

[2] Zhang LJ, Xu ZM, Guo JY, Dai SM, Dang H, Lü S, et al. [Endemic status of schistosomiasis in People's Republic of China in 2018]. Zhongguo Xue Xi Chong Bing Fang Zhi Za Zhi. 2019;31(6):576-82.

[3] Chuah C, Jones MK, Burke ML, McManus DP, Gobert GN. Cellular and chemokine-mediated regulation in schistosome-induced hepatic pathology. Trends Parasitol. 2014;30(3):141-50.

[4] Dulak J, Szade K, Szade A, Nowak W, Józkowicz A. Adult stem cells: hopes and hypes of regenerative medicine. Acta Biochim Pol. 2015;62(3):329-37.

[5] Dai Z, Song G, Balakrishnan A, Yang T, Yuan Q, Möbus S, et al. Growth differentiation factor 11 attenuates liver fibrosis via expansion of liver progenitor cells. Gut. 2020;69(6):1104-15.

[6] Lukacs-Kornek V, Lammert F. The progenitor cell dilemma: Cellular and functional heterogeneity in assistance or escalation of liver injury. J Hepatol. 2017;66(3):619-30.

[7] Liu J, Zhu L, Wang J. Schistosoma japonicum extracellular vesicle miRNA cargo regulates host macrophage functions facilitating parasitism. PLoS Pathog. 2019;15(6):e1007817.

[8] Carson JP, Ramm GA, Robinson MW, McManus DP, Gobert GN. Schistosome-Induced Fibrotic Disease: The Role of Hepatic Stellate Cells. Trends Parasitol. 2018;34(6):524-40.

[9] Spee B, Carpino G, Schotanus BA, Katoonizadeh A, Vander Borght S, Gaudio E, et al. Characterisation of the liver progenitor cell niche in liver diseases: potential involvement of Wnt and Notch signalling. Gut. 2010;59(2):247-57.

[10] Nobili V, Carpino G, Alisi A, Franchitto A, Alpini G, De Vito R, et al. Hepatic progenitor cells activation, fibrosis, and adipokines production in pediatric nonalcoholic fatty liver disease. Hepatology. 2012;56(6):2142-53.

[11] Zhang B, Wu X, Liu J, Song L, Song Q, Wang L, et al. β-Actin: Not a Suitable Internal Control of Hepatic Fibrosis Caused by Schistosoma japonicum. Front Microbiol. 2019;10:66.

[12] Ko S, Russell JO, Molina LM, Monga SP. Liver Progenitors and Adult Cell Plasticity in Hepatic Injury and Repair: Knowns and Unknowns. Annu Rev Pathol. 2020;15:23-50.

[13] Teufelberger AR, Nordengrün M, Braun H, Maes T, De Grove K, Holtappels G, et al. The IL-33/ST2 axis is crucial in type 2 airway responses induced by Staphylococcus aureus-derived serine protease-like protein D. J Allergy Clin Immunol. 2018;141(2):549-59.e7.

[14] Vasanthakumar A, Kallies A. Interleukin (IL)-33 and the IL-1 Family of Cytokines-Regulators of Inflammation and Tissue Homeostasis. Cold Spring Harbor perspectives in biology. 2019;11(3).

[15] Song Z, Gupta K, Ng IC, Xing J, Yang YA, Yu H. Mechanosensing in liver regeneration. Semin Cell Dev Biol. 2017;71:153-67.

[16] Gryseels B, Polman K, Clerinx J, Kestens L. Human schistosomiasis. Lancet. 2006;368(9541):1106-18.

[17] Aizarani N, Saviano A, Sagar, Mailly L, Durand S, Herman JS, et al. A human liver cell atlas reveals heterogeneity and epithelial progenitors. Nature. 2019;572(7768):199-204.

[18] Raven A, Forbes SJ. Hepatic progenitors in liver regeneration. J Hepatol. 2018;69(6):1394-5.

[19] Itoh T. Stem/progenitor cells in liver regeneration. Hepatology. 2016;64(2):663-8.

[20] Tirnitz-Parker JEE, Forbes SJ, Olynyk JK. Cellular Plasticity in Liver Regeneration: Spotlight on Cholangiocytes. Hepatology. 2019;69(5):2286-9.

[21] Kaur S, Siddiqui H, Bhat MH. Hepatic Progenitor Cells in Action: Liver Regeneration or Fibrosis? Am J Pathol. 2015;185(9):2342-50.

[22] Chen J, Chen L, Zern MA, Theise ND, Diehl AM, Liu P, et al. The diversity and plasticity of adult hepatic progenitor cells and their niche. Liver Int. 2017;37(9):1260-71.

[23] Lanzoni G, Cardinale V, Carpino G. The hepatic, biliary, and pancreatic network of stem/progenitor cell niches in humans: A new reference frame for disease and regeneration. Hepatology. 2016;64(1):277-86.

[24] Mao Y, Tang S, Yang L, Li K. Inhibition of the Notch Signaling Pathway Reduces the Differentiation of Hepatic Progenitor Cells into Cholangiocytes in Biliary Atresia. Cell Physiol Biochem. 2018;49(3):1074-82.

[25] Ma Z, Li F, Chen L, Gu T, Zhang Q, Qu Y, et al. Autophagy promotes hepatic differentiation of hepatic progenitor cells by regulating the Wnt/β-catenin signaling pathway. J Mol Histol. 2019;50(1):75-90.

[26] Xu H, Qian H, Zhu W, Zhang X, Yan Y, Mao F, et al. Mesenchymal stem cells relieve fibrosis of Schistosoma japonicum-induced mouse liver injury. Exp Biol Med (Maywood). 2012;237(5):585-92.

[27] You Y, Wen DG, Gong JP, Liu ZJ. Research Status of Mesenchymal Stem Cells in Liver Transplantation. Cell Transplantation. 2019;28(12):1490-506.

[28] Lou G, Chen Z, Zheng M, Liu Y. Mesenchymal stem cell-derived exosomes as a new therapeutic strategy for liver diseases. Exp Mol Med. 2017;49(6):e346.

[29] De Salvo C, Pastorelli L, Petersen CP, Buttò LF, Buela KA, Omenetti S, et al. IL-33 triggers early eosinophil-dependent events leading to metaplasia in a chronic model of gastritis-prone mice. Gastroenterology. 2020.

[30] Sun Z, Chang B, Gao M, Zhang J. IL-33-ST2 Axis in Liver Disease: Progression and Challenge. Mediators Inflamm. 2017;2017:5314213.

[31] Peng H, Zhang Q, Li X, Liu Z, Shen J, Sun R, et al. IL-33 Contributes to Schistosoma japonicum-induced Hepatic Pathology through Induction of M2 Macrophages. Sci Rep. 2016;6:29844.

[32] He X, Xie J, Wang Y, Fan X, Su Q, Sun Y, et al. Down-regulation of microRNA-203-3p initiates type 2 pathology during schistosome infection via elevation of interleukin-33. PLoS Pathog. 2018;14(3):e1006957.

[33] Kitade M, Kaji K, Yoshiji H. Relationship between hepatic progenitor cell-mediated liver regeneration and non-parenchymal cells. Hepatol Res. 2016;46(12):1187-93.

Figures

Figure 1

The dynamic of histopathological changes and liver regeneration in a single infection mouse model with S. japonicum. (A) Representative images of HE staining at different infection time points. Arrows indicate the necrosis. (B) The statistical analysis of percents of granulomas area. n = 5-7 mice/group. (C) Representative images of Masson staining. (D) The statistical analysis of percents of fibrosis area. n = 5-7 mice/group. (E) Representative images of Tunel staining. n = 3 mice/group. (F) Representative images of CD45 staining. n = 3 mice/group. (G) Representative images of F4/80 staining. n = 3 mice/group. (H) The expression level of Albumin in serum. n = 5-7 mice/group. Images were captured by an inverted microscope (Olympus, BX63, Tokyo, Japan). *P < 0.05; **P < 0.01, ***P <0.001.

Figure 2

The expansion of HPCs was induced in mice with S. japonicum. infection. Representative images of A6 staining (A), CK19 staining (B) and Epcam staining (C). The statistical analysis of A6 positive cells per area (D), CK19 positive cells per area (E) and Epcam positive cells per area (F). n = 4 mice/group. (G) Relative HGF mRNA level in livers. n = 4 mice/group. (H) Relative IL-6 mRNA level in livers. n = 4 mice/group. *P < 0.05; **P < 0.01, ***P <0.001.

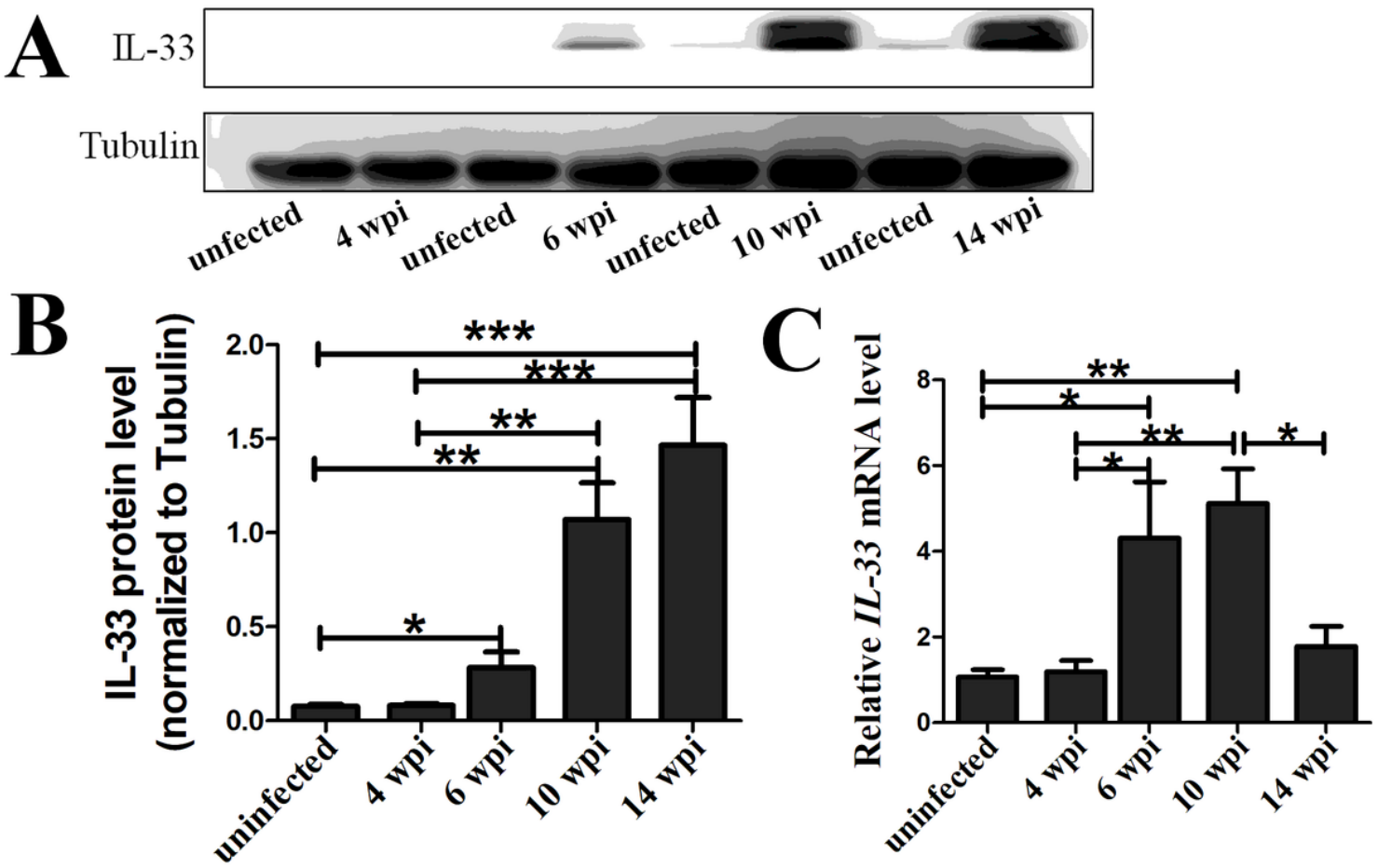

Figure 5

The dynamic change of IL-33 in S. japonicum infection mice model. (A) Representative bands of IL-33 protein by western blot. (B) The statistical analysis of the IL-33 protein. n = 4 mice/group. (C) Real-time PCR analysis of IL-33 mRNA. n = 5 mice/group. *P < 0.05; **P < 0.01, ***P <0.001.

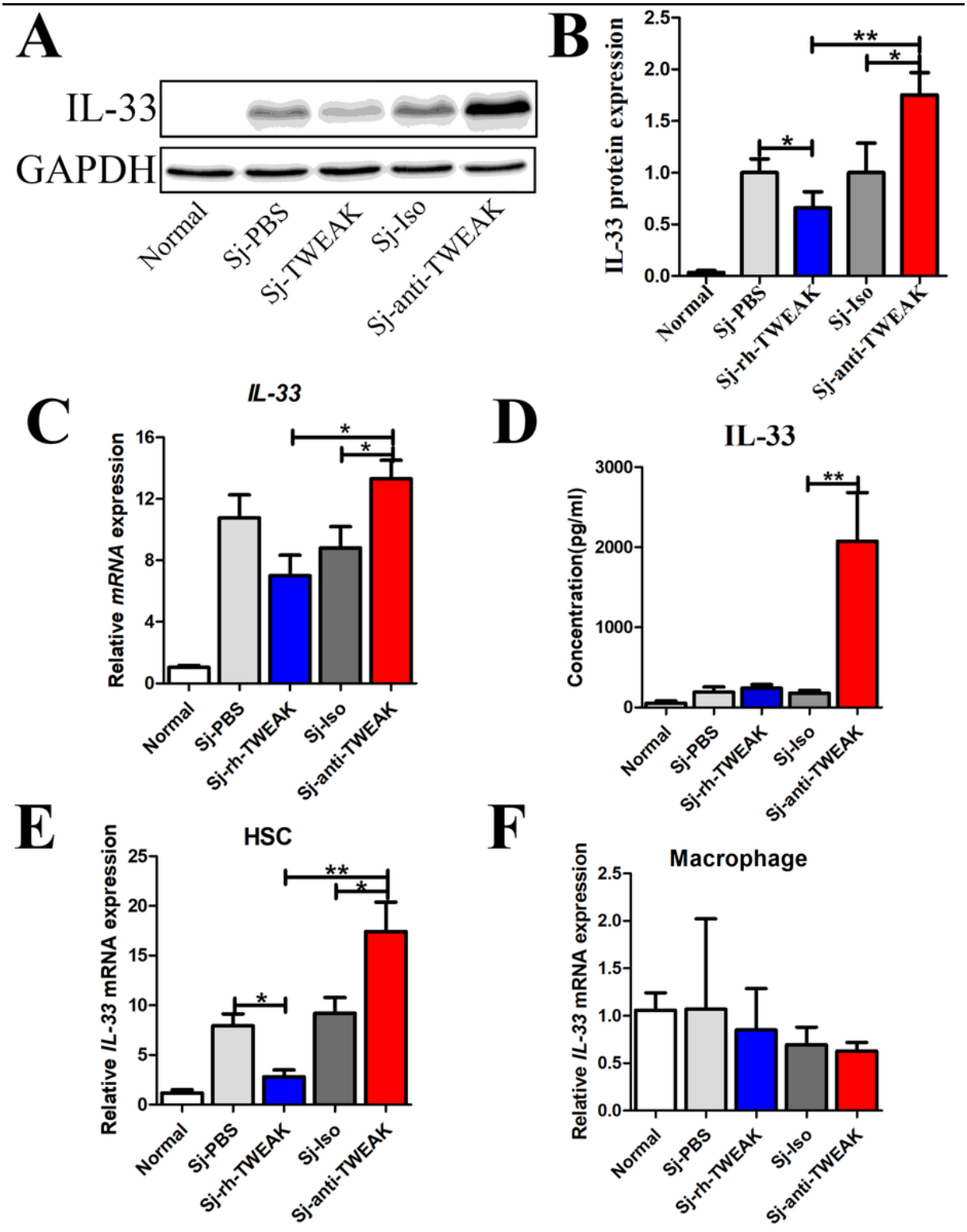

Figure 6

HPCs inhibited IL-33 secretion in S. japonicum infection mice liver. (A) Representative bands of IL-33 protein by western blot in different groups. (B) The statistical analysis of the IL-33 protein. n = 4 mice/group. (C) Real-time PCR analysis of IL-33 mRNA in the liver. n = 5 mice/group. (D) ELISA analysis of the concentration of IL-33 in serum. n = 4 mice/group. (E) Real-time PCR analysis of IL-33 mRNA in

HSC. n = 4 mice/group. (F) Real-time PCR analysis of IL-33 mRNA in macrophage. n = 4 mice/group.*P < 0.05; **P < 0.01.